PAN
ARCHIVES OF ACOUSTICS
Vol. **46**, No. 1, pp. 17–24 (2021)
DOI: 10.24425/aoa.2021.136556

Research Paper

New Theoretical Model for Mass Sensitivity of Love Wave Sensors

Piotr KIEŁCZYŃSKI*, Marek SZALEWSKI, Andrzej BALCERZAK, Krzysztof WIEJA

Institute of Fundamental Technological Research
Polish Academy of Sciences
Warsaw, Poland
*Corresponding Author e-mail: pkielczy@ippt.pan.pl

(*received July 29, 2020; accepted September 25, 2020*)

In this work we analyse basic characteristics of Love wave sensors implemented in waveguide structures composed of a lossy viscoelastic surface layer deposited on a lossless elastic substrate. It has to be noted that Love wave sensors working at ultrasonic frequencies have the highest mass density sensitivity $S_\sigma^{v_p}$ among all known ultrasonic sensors, such as QCM, Lamb wave or Rayleigh wave sensors. In this paper we have established an exact analytical formula for the mass density sensitivity $S_\sigma^{v_p}$ of the Love wave sensors in the form of an explicit algebraic expression. Subsequently, using this developed analytical formula, we compared theoretically the mass density sensitivity $S_\sigma^{v_p}$ for various Love wave waveguide structures, such as: (1) lossy PMMA surface layer on lossless Quartz substrate and (2) lossy PMMA on lossless Diamond substrate. The performed analysis shows that the mass density sensitivity $S_\sigma^{v_p}$ (real and imaginary part) for a sensor with a structure PMMA on Diamond is five times higher than that of a PMMA on Quartz structure. It was found that the mass density sensitivity $S_\sigma^{v_p}$ for Love wave sensors increases with the increase of the ratio: bulk shear wave velocity in the substrate to bulk shear wave velocity in the surface layer.

Keywords: Love wave sensors; mass sensitivity; complex dispersion equation; viscoelastic layers.

1. Introduction

Ultrasonic waves (bulk and surface), widely used in sensing applications, have been successfully employed in a variety of sensors, such as biosensors, chemosensors, and other sensors measuring large number of physical quantities, e.g. humidity, viscosity, etc. (Ballantine *et al.*, 1997; Pajewski *et al.*, 1998; Kiełczyński *et al.*, 1998; 2014a; 2014b; 2015a; Rocha Gaso *et al.*, 2013; Vikström, Voinova, 2016). Sensors which utilise surface waves of the Love type offer many advantages over the sensors employing other types of ultrasonic waves (Chen, Liu, 2010; Kiełczyński, Szalewski, 2011; Kiełczyński *et al.*, 2014b; 2014c; Wu *et al.*, 2017; Kiełczyński, 2018; Takayanagi, Kondoh, 2018; El Baroudi, Pommellec, 2019). Of all types of ultrasonic waves, Love waves are the most predestined to be used for constructing sensors of physical quantities, chemosensors, and biosensors.

Shear horizontal surface Love waves have only one component of the mechanical displacement, which attains the highest value at the waveguide surface and diminishes with the increase of the distance from the surface into the bulk of the waveguide.

Energy of ultrasonic Love waves is concentrated in the vicinity of the waveguide surface. From this reason, Love waves are very sensitive to the changes of physical properties that occur at the surface layer.

The mass density sensitivity $S_\sigma^{v_p}$ is one of the most important parameters characterising operation and applicability of the ultrasonic sensor, for measurements in liquid environment. In design of Love wave sensors we seek to find a sensor's configuration for which the output of the sensor is significantly altered by presence of an extra mass layer loading the upper surface of the sensor's waveguide. In fact, large changes in ultrasonic velocity Δv_p and/or attenuation $\Delta\alpha$ of the Love wave will lead to higher accuracy of measurements with Love wave sensors. In Love wave biosensors, working in a liquid environment, a thin mass layer can be built on the sensor surface due to interactions of the initially deposited recognition layer with an investigated analyte, extracted directly from the surrounding liquid.

In this work, we have performed theoretical analysis and numerical calculations for the mass density sensitivity $S_\sigma^{v_p}$ of Love wave sensors, operating at ultrasonic frequencies. In this paper, on the upper propagation surface of the Love wave waveguide an infinitesimally thin film with surface mass density σ is attached. The presence of this layer alters the propagation characteristics (i.e., phase velocity) of the Love wave. Love wave sensors show the highest sensitivity to mass load, compared to sensors using other acoustic (surface and bulk) waves, e.g., Lamb waves or Rayleigh waves.

Mass sensitivity is a fundamental parameter that determines the quality of the ultrasonic Love wave sensors. Up to date, the mass density sensitivity $S_\sigma^{v_p}$ of Love wave sensors has been determined only approximately employing a number of simplifying assumptions.

In this work, we derive for the first time the mass density sensitivity $S_\sigma^{v_p}$ of Love wave sensors in the form of an exact analytical formula, without referring to any simplifications and limitations.

An analytical formula for the mass density sensitivity $S_\sigma^{v_p}$ has a huge advantage due to its capability to reveal explicitly functional dependencies of the sensitivity $S_\sigma^{v_p}$ as a function of all material and geometrical parameters of the Love wave waveguide, such as moduli of elasticity and density of the surface layer and substrate, thickness of the surface layer, as well as wave frequency. Such an insight cannot be easily achieved with pure numerical methods. Therefore, the necessity for labourious and extensive numerical calculations has been greatly reduced.

2. Physical model

2.1. Geometry of the Love wave waveguide

In this paper we analyse Love waves that propagate in the following layered waveguides: (1) PMMA surface layer deposited on the semi-infinite ST-cut Quartz substrate and (2) PMMA surface layer deposited on the semi-infinite diamond substrate, see Fig. 1. Material and geometrical parameters of these two layered waveguides are given in Table 1.

The layered Love wave waveguide structure, analysed in this paper (see Fig.1) represents a physical model of the Love wave sensor.

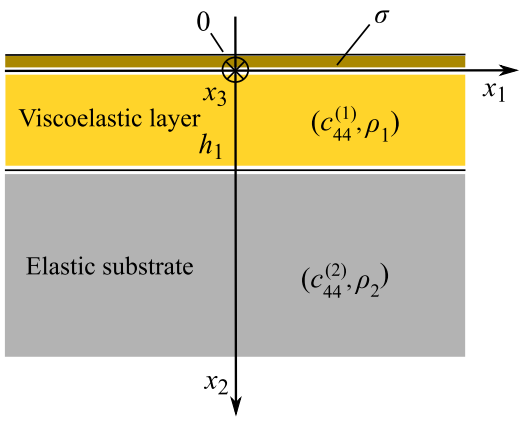

Fig. 1. Cross-section of the analysed Love wave waveguide loaded with a surface mass density σ. Love surface waves propagate along the x_1 axis. Shear horizontal (SH) mechanical displacement u_3 of the Love wave is directed along the x_3 axis.

The waveguide is designed to support shear horizontal (SH) surface waves of the Love type when the phase velocity of shear ultrasonic waves in the surface layer is lower than that in the substrate. The composite waveguide consists of a lossy viscoelastic surface layer ($h_1 > x_2 \geq 0$) which is rigidly bonded to a lossless infinite elastic substrate occupying the lower half-space ($x_1 > h_2$).

The lossy surface layer being a viscoelastic material, such as PMMA (PolyMethyl Methacrylate), is characterised by a complex shear modulus of elasticity $c_{44}^{(1)} = c_1 - j\omega\eta_{44}$ (Kelvin-Voigt model). By contrast, the lossless substrate is a semi-infinite elastic medium, such as ST-cut Quartz and/or Diamond, with real shear modulus of elasticity equal to $c_{44}^{(2)}$. It is well known from previous research that the above materials can support pure SH bulk waves (Liu *et al.*, 2015; Xu, Juan, 2018) with no spurious components of vibrations along x_1 and x_2 axes.

A unique vibration pattern of Love surface waves is an important property. In fact, Love surface waves have only one non-zero shear-horizontal (SH) component of the mechanical displacement u_3, which is directed along the x_3 axis, parallel to the free surface ($x_2 = 0$) of the waveguide and perpendicular to the direction of the Love wave propagation along the x_1 axis.

Table 1. Material and geometrical parameters of Love wave waveguides (Rasmusson, Gizeli, 2001; Kushibiki *et al.*, 2002; Raum, Brandt, 2003; Chu *et al.*, 2003; Mortet *et al.*, 2008).

Material	Thickness [μm]	Density [kg/m^3]	Storage shear modulus [GPa]	SH wave velocity [m/s]	Compressional wave velocity [m/s]	Viscosity [Pa·s]
PMMA surface layer	$h_1 = 1 - 10$	$\rho_1 = 1180$	$c_1 = 1.43$	$v_1^0 = 1100$	$v_1^L = 2667$	$\eta_{44} = 0.37$
ST-cut quartz substrate	semi-infinite	$\rho_2 = 2650$	$c_{44}^{(2)} = 67.85$	$v_2 = 5060$	$v_2^L = 7032$	0
Diamond substrate	semi-infinite	$\rho_2 = 3515$	$c_{44}^{(2)} = 578$	$v_2 = 12\,823$	$v_2^L = 17\,520$	0

The x_2 axis is directed into the bulk of the substrate. All material parameters of the composite waveguide may change only along the x_2 axis but are homogeneous and isotropic along the x_1 and x_3 axes.

A Love wave that propagates in a lossy layered waveguide from Fig.1 undergoes attenuation. Consequently, the wave number k of the Love wave is a complex quantity:

$$k = k_0 + j\alpha, \tag{1}$$

where $j = \sqrt{-1}$ is the imaginary unit, k_0 is the real part of the complex wavenumber which determines the phase velocity of the Love wave propagation, α is the attenuation of the Love wave, and ω is the angular frequency.

3. Mathematical model

The Love wave propagating in the waveguide structure from Fig. 1 is governed by the appropriate equations of motion (Achenbach, 1973; Rose, 2014) in the constituent regions and the appropriate boundary conditions (Auld, 1990) on the upper and lower surfaces of the surface layer.

3.1. Governing equations of motion

3.1.1. Lossy viscoelastic surface layer ($h_1 > x_2 > 0$)

The mechanical displacement $u_3^{(1)}$ of the Love wave in the viscoelastic surface layer fulfills the following equation of motion:

$$\frac{1}{v_1^2}\frac{\partial^2 u_3^{(1)}}{\partial t^2} = \frac{\partial^2 u_3^{(1)}}{\partial x_1^2} + \frac{\partial^2 u_3^{(1)}}{\partial x_2^2}, \tag{2}$$

where

$$v_1 = \left(\frac{c_1 - j\omega\eta_{44}}{\rho_1}\right)^{1/2} = v_1^0\left(1 - \frac{j\omega\eta_{44}}{c_1}\right)^{1/2}$$

is the complex bulk SH wave velocity in the first viscoelastic surface layer, c_1 is its storage modulus, ρ_1 is the density of the viscoelastic surface layer, η_{44} is its viscosity, $v_1^0 = (c_1/\rho_1)^{1/2}$ is the velocity of the bulk SH wave in the lossless elastic surface layer (for $\eta_{44} = 0$).

3.1.2. Semi-infinitive elastic substrate ($x_2 > h_1$)

The mechanical displacement $u_3^{(2)}$ of the Love wave in the elastic substrate satisfies the following partial differential equation (equation of motion):

$$\frac{1}{v_2^2}\frac{\partial^2 u_3^{(2)}}{\partial t^2} = \frac{\partial^2 u_3^{(2)}}{\partial x_1^2} + \frac{\partial^2 u_3^{(2)}}{\partial x_2^2}, \tag{3}$$

where $v_2 = \left(c_{44}^{(2)}/\rho_2\right)^{1/2}$ is the velocity of the bulk SH wave in the elastic substrate, $c_{44}^{(2)}$ its storage modulus of elasticity, and ρ_2 is the density in the elastic substrate.

3.2. Thomson-Haskell Transfer Matrix method

Complex dispersion equation of Love surface waves propagating in the lossy waveguide presented in Fig. 1 has been derived in this paper using Thomson-Haskell Transfer Matrix method (Thomson, 1950; Haskell, 1953; Ke *et al.,* 2011).

The key element in the Thomson-Haskell method is to relate mechanical displacement and shear stress of the Love wave on the upper surface of each layer with mechanical displacement and shear stress on the lower surface of the considered layer. Below we show briefly the derivation of this relationship.

A general form of the time-harmonic solution for the equations of motion (Eqs (2) and (3)) in the subsequent layers corresponding to a time-harmonic Love surface wave is sought in the following form:

$$u_3(x_1, x_2, t) = V(x_2)\cdot\exp\left[j\left(kx_1 - \omega t\right)\right], \tag{4}$$

where $V(x_2)$ is the transverse distribution of the mechanical displacement u_3 of the Love surface wave as a function of depth x_2, k is the complex wave number of the Love wave.

The shear stress associated with the mechanical displacement u_3 of the Love wave is given by the following formula:

$$\tau_{23}\left(x_1, x_2, t\right) = T(x_2)\cdot\exp\left[j\left(kx_1 - \omega t\right)\right], \tag{5}$$

where

$$T(x_2) = c_{44}(x_2)\frac{\partial V(x_2)}{\partial x_2}.$$

Here $c_{44}(x_2)$ is the shear modulus of elasticity of the material in the constituent parts of the waveguide.

Taking into account Eq. (4), the equation of motion (see Eqs (2) and (3)) for the subsequent layer is reduced to an ordinary differential equation of the second order. Considering two new dependent variables (V and T), each of the second order differential equations resulting from Eqs (2) and (3) can be represented as a system of two differential equations of the first order, namely:

$$\frac{d}{dx}\begin{bmatrix} V \\ T \end{bmatrix} = \begin{bmatrix} 0, & \dfrac{1}{c_{44}(x)} \\ \beta^2 c_{44}(x) - \omega^2\rho(x), & 0 \end{bmatrix}\begin{bmatrix} V \\ T \end{bmatrix}. \tag{6}$$

Solving this matrix differential equation (6), for example for the PMMA surface layer, we arrive at the following formula (Eq. (7)) linking mechanical displacement and shear stress on the upper surface of the PMMA layer for ($x_2 = 0$) with mechanical displacement and shear stress on the lower surface of this layer for ($x_2 = h_1$). Details of this derivation are given in (Kiełczyński *et al.,* 2016)

$$\left[\begin{matrix} V \\ T \end{matrix}\right]\Bigg|_{x=h_1} = \cos(q_1 \cdot h_1) \cdot \left[\begin{matrix} 1, & \dfrac{1}{c_{44}^{(1)} \cdot q_1} \tan(q_1 \cdot h_1) \\ -c_{44}^{(1)} \cdot q_1 \cdot \tan(q_1 \cdot h_1), & 1 \end{matrix}\right] \cdot \left[\begin{matrix} V \\ T \end{matrix}\right]\Bigg|_{x=0} = \left[\begin{matrix} A_{11} & A_{12} \\ A_{21} & A_{22} \end{matrix}\right] \cdot \left[\begin{matrix} V \\ T \end{matrix}\right]\Bigg|_{x=0}, \tag{7}$$

where $q_1 = \sqrt{k_1^2 - k^2}$ is the transverse wavenumber of the Love wave in the first PMMA surface layer, $k_1 = \frac{\omega}{v_1}$, v_1 is the complex phase velocity of bulk SH waves in the PMMA surface layer, $k = k_0 + j\alpha$ is the complex wave number of the Love wave, and $[A]$ is the transfer matrix.

The transfer matrix $[A]$ in Eq. (7) can be expressed as:

$$[A] = \left[\begin{matrix} A_{11} & A_{12} \\ A_{21} & A_{22} \end{matrix}\right] = \left[\begin{matrix} \cos(q_1 \cdot h_1) & \dfrac{1}{c_{44}^{(1)} \cdot q_1} \sin(q_1 \cdot h_1) \\ -c_{44}^{(1)} \cdot q_1 \cdot \sin(q_1 \cdot h_1) & \cos(q_1 \cdot h_1) \end{matrix}\right]. \tag{8}$$

The unknown components of the mechanical displacement and the corresponding shear stress of the Love wave at the interface $x_2 = 0$ and $x_2 = h_1$ will be further denoted by V_0, T_0 and V_D, T_D, respectively,

$$\left[\begin{matrix} V_D \\ T_D \end{matrix}\right] = \left[\begin{matrix} A_{11} & A_{12} \\ A_{21} & A_{22} \end{matrix}\right] \left[\begin{matrix} V_0 \\ T_0 \end{matrix}\right]. \tag{9}$$

3.3. Shear stresses on top and bottom of the first surface layer No. 1

The top surface of the first PMMA layer No. 1 ($x_2 = 0$) is loaded with an infinitesimally thin layer with the surface mass density σ.

The shear stress of the SH Love wave in this infinitesimally thin layer at the interface with the PMMA surface layer No. 1 is given by:

$$T_0 = -\sigma \cdot \omega^2 V_0. \tag{10}$$

This dependence results from the Newton's second principle of motion.

The bottom of the viscoelastic surface layer No. 1 (PMMA) ($x_2 = h_1$) is rigidly bonded to the semi-infinite elastic substrate (material No. 2). The dependence of the mechanical displacement on the depth $V(x_2)$ in an elastic substrate is given by $V(x_2) = V_D \cdot \exp(-b \cdot x_2)$. Therefore, the shear stress in the elastic substrate at the interface with the viscoelastic surface layer No. 1 (PMMA) is given by:

$$T_D = c_{44}^{(2)} \frac{\partial V}{\partial x_2}\Big|_{(x_2=h_1)} = -c_{44}^{(2)} \cdot b \cdot V_D, \tag{11}$$

where $b = (k^2 - k_2^2)^{1/2}$, $k_2 = \frac{\omega}{v_2}$, $v_2 = \left(\frac{c_{44}^{(2)}}{\rho_2}\right)^{1/2}$. The parameters b and k_2 correspond, respectively, to the transverse wavenumber of the Love surface wave in the substrate and the wavenumber of bulk SH waves in the substrate.

Substituting values of the shear stresses T_0 and T_D given by Eqs (10) and (11) into Eq. (9) leads to:

$$\left[\begin{matrix} V_D \\ -c_{44}^{(2)} \cdot b \cdot V_D \end{matrix}\right]\Bigg|_{x=h_1} = \left[\begin{matrix} A_{11} & A_{12} \\ A_{21} & A_{22} \end{matrix}\right] \cdot \left[\begin{matrix} V_0 \\ -\sigma \cdot \omega^2 \cdot V_0 \end{matrix}\right]\Bigg|_{x=0}. \tag{12}$$

In fact, Eq. (12) contains only two unknowns: V_0 and V_D. By a simple rearrangement of the terms, Eq. (12) can be written as:

$$\left[\begin{matrix} 1, & -\left(A_{11} - A_{12} \cdot \sigma \cdot \omega^2\right) \\ c_{44}^{(2)} \cdot b, & \left(A_{21} - A_{22} \cdot \sigma \cdot \omega^2\right) \end{matrix}\right] \cdot \left[\begin{matrix} V_D \\ V_0 \end{matrix}\right] = \left[\begin{matrix} 0 \\ 0 \end{matrix}\right]. \tag{13}$$

3.4. Complex dispersion equation

A necessary condition for the existence of a non-zero solution of Eq. (13) requires zeroing of the determinant of the 2×2 matrix in Eq. (13). This condition leads to the following complex dispersion equation for Love waves:

$$\left(A_{21} - A_{22} \cdot \sigma \cdot \omega^2\right) + \left(c_{44}^{(2)} \cdot b\right) \cdot \left(A_{11} - A_{12} \cdot \sigma \cdot \omega^2\right) = 0. \tag{14}$$

Substituting into Eq. (14) the elements of the matrix $[A]$ given by Eq. (8), we arrive finally at the following complex dispersion equation for the Love surface waves propagating in the lossy composite waveguide, shown in Fig. 1:

$$\tan(q_1 \cdot h_1) \cdot \left\{\left(c_{44}^{(1)} \cdot q_1\right)^2 + \left(\sigma \cdot \omega^2\right) \cdot \left(c_{44}^{(2)} \cdot b\right)\right\} + \left(c_{44}^{(1)} \cdot q_1\right) \cdot \left\{\left(\sigma \cdot \omega^2\right) - \left(c_{44}^{(2)} \cdot b\right)\right\} = 0, \tag{15}$$

where $k_1 = \frac{\omega}{v_1}$, $k_2 = \frac{\omega}{v_2}$, $q_1 = \sqrt{k_1^2 - k^2}$, $b = \sqrt{k^2 - k_2^2}$, σ is the surface mass density loading the surface of the waveguide, and k is the complex wavenumber of the Love wave.

Equation (15) constitutes the mathematical model of the propagation of Love waves in the waveguide structure from Fig. 1. Equation (15) relates the phase velocity and attenuation of the Love wave propagating in the waveguide with material and geometrical parameters of the layered waveguide, depicted in Fig. 1. It should be stressed upon that an extra mass loading does not introduce any extra losses but only changes in the phase velocity of the Love wave.

The complex dispersion equation (Eq. (15)) can be written in a more abstract form as

$$\mathbf{F}\left(c_{44}^{(1)}, \rho_1, c_{44}^{(2)}, \rho_2, \eta_{44}, \sigma, h_1, \omega;\ k_0, \alpha\right) = 0, \tag{16}$$

where the bolded symbol **F** denotes that the equation is defined in the complex domain.

The complex dispersion equation (Eq. (16)) was subsequently split into its real and imaginary parts $\mathrm{Re}\,\mathbf{F}$ and $\mathrm{Im}\,\mathbf{F}$, which were further equated to zero, namely:

$$\mathrm{Re}\,\mathbf{F}\left(c_{44}^{(1)},\,\rho_1,\,c_{44}^{(2)},\,\rho_2,\,\eta_{44},\,\sigma,\,h_1,\,\omega;\;k_0,\,\alpha\right)=0, \quad (17)$$

$$\mathrm{Im}\,\mathbf{F}\left(c_{44}^{(1)},\,\rho_1,\,c_{44}^{(2)},\,\rho_2,\,\eta_{44},\,\sigma,\,h_1,\,\omega;\;k_0,\,\alpha\right)=0. \quad (18)$$

Equations (17) and (18) constitute a system of two nonlinear transcendental algebraic equations for two unknowns k_0 and α. The parameters in Eqs (17) and (18) are the following: $c_{44}^{(1)}$, ρ_1, $c_{44}^{(2)}$, ρ_2, η_{44}, σ, h_1, and ω. It is rather unrealistic to expect that any closed form solution for the system of two algebraic Eqs (17) and (18) would emerge. Therefore, the nonlinear system of two algebraic Eqs (17) and (18) has to be solved numerically.

The system of two nonlinear algebraic Eqs (17) and (18) was solved numerically using specialised procedures from the computer package Scilab.

The solution of this set of nonlinear algebraic equations (Eqs (17) and (18)) provides the complex wave number $k = k_0 + j\alpha$ of the Love wave.

4. Sensitivity to mass loading $S_\sigma^{v_p}$

The sensitivity $S_\sigma^{v_p}$ of the Love wave sensor to the surface density mass loading can be defined as follows (Ballantine *et al.*, 1997):

$$S_\sigma^{v_p}=\frac{1}{v_p}\left(\frac{\mathrm{d}v_p}{\mathrm{d}\sigma}\right). \quad (19)$$

For lossy waveguide structures, the phase velocity of the Love wave can be defined as a complex quantity: $v_p = \omega/k$. As a result, the mass density sensitivity defined by Eq. (19) becomes also a complex quantity.

4.1. Exact analytical solution for mass sensitivity

Dispersion Eq. (15) can be regarded as an implicit function $F(v_p, \sigma) = 0$ of the phase velocity v_p and surface mass density σ which loads the waveguide surface. The derivative $\frac{\mathrm{d}v_p}{\mathrm{d}\sigma}$ in formula (19) can be calculated by applying the theorem of differentiation of implicit function, namely:

$$\frac{\mathrm{d}v_p}{\mathrm{d}\sigma}=-\frac{\partial F/\partial\sigma}{\partial F/\partial v_p}. \quad (20)$$

As a consequence of employing Eqs (19) and (20) we have derived for the first time the following explicit formula for the mass density sensitivity $S_\sigma^{v_p}$:

$$S_\sigma^{v_p}=\frac{\omega^2\dfrac{1}{k}\left\{\left(c_{44}^{(1)}q_1\right)+\left(c_{44}^{(2)}b\right)\cdot\tan\left(q_1h_1\right)\right\}}{a^*}, \quad (21)$$

where

$$a^*=\frac{h_1}{\cos^2\left(q_1h_1\right)}\frac{\partial q_1}{\partial k}\left\{\left(c_{44}^{(1)}q_1\right)^2+\left(c_{44}^{(2)}b\right)\left(\sigma\omega^2\right)\right\}$$
$$+\tan\left(q_1h_1\right)\left\{2q_1\left(c_{44}^{(1)}\right)^2\frac{\partial q_1}{\partial k}+c_{44}^{(2)}\frac{\partial b}{\partial k}\left(\sigma\omega^2\right)\right\}$$
$$+c_{44}^{(1)}\frac{\partial q_1}{\partial k}\cdot\left\{\left(\sigma\omega^2\right)-\left(c_{44}^{(2)}b\right)\right\}-c_{44}^{(2)}\frac{\partial b}{\partial k}\left(c_{44}^{(1)}q_1\right),$$

$$\frac{\partial q_1}{\partial k}=-\frac{k}{\sqrt{k_1^2-k^2}},\qquad \frac{\partial b}{\partial k}=\frac{k}{\sqrt{k^2-k_2^2}}$$

and k is the complex wave number of the Love wave.

Equation (21) is an exact analytical formula for the mass density sensitivity $S_\sigma^{v_p}$ of Love wave sensors presented in Fig. 1.

Equation (21) will be further used in the subsequent numerical calculations of the mass density sensitivity $S_\sigma^{v_p}$ of the Love wave sensors.

5. Results

Using the derived analytical formula (Eq. (21)) we have calculated numerically the real part of the mass density sensitivity $S_\sigma^{v_p}$ of the Love wave sensor, for various combinations of the surface layer and substrate materials. As a substrate material, ST-cut Quartz and Diamond were chosen.

Firstly, the real part of the mass density sensitivity $S_\sigma^{v_p}=\frac{1}{v_p}\left(\frac{dv_p}{d\sigma}\right)$, as a function of frequency f of the Love surface wave and thickness h_1 of PMMA guiding surface layer is given, respectively, in Figs 2 and 3. Here, as a substrate we chose an ST-cut Quartz material. The following surface mass density at the sensor operating point has been chosen: $\sigma = 1\cdot10^{-6}$ kg/m^2.

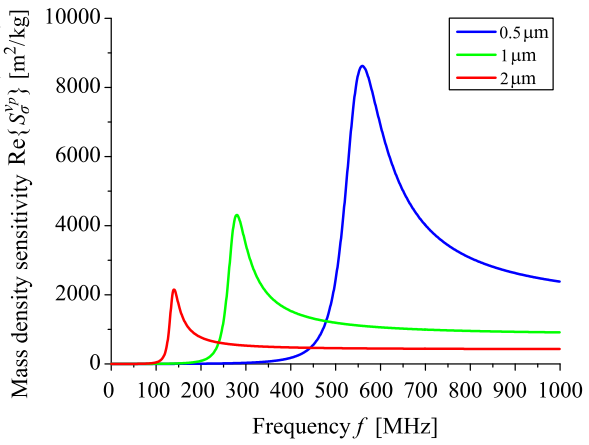

Fig. 2. Real part of the mass density sensitivity $S_\sigma^{v_p}$ [m^2/kg] for Love surface waves propagating in PMMA-ST – Quartz waveguides loaded with a thin lossless film with the surface mass density σ, as a function of Love wave frequency f, for different values of thickness h_1 of the guiding PMMA surface layer (h_1 = 0.5, 1, and 2 µm).

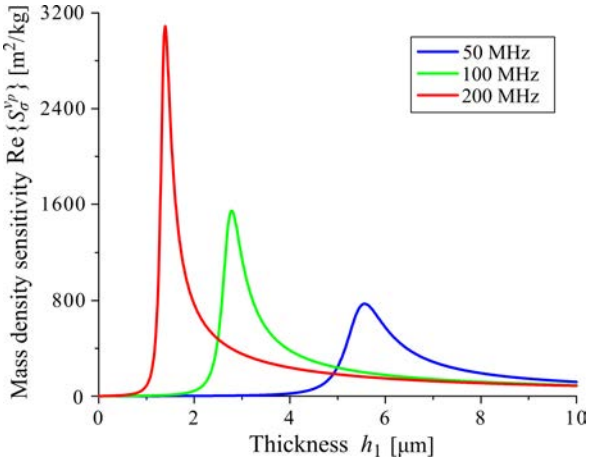

Fig. 3. Real part of the mass density sensitivity $S_\sigma^{v_p}$ [m^2/kg] for Love surface waves propagating in PMMA-ST – Quartz waveguides, loaded with a thin lossless film with the mass density σ, as a function of thickness h_1 of the PMMA guiding surface layer, for different values of wave frequency f = 50, 100, and 200 MHz.

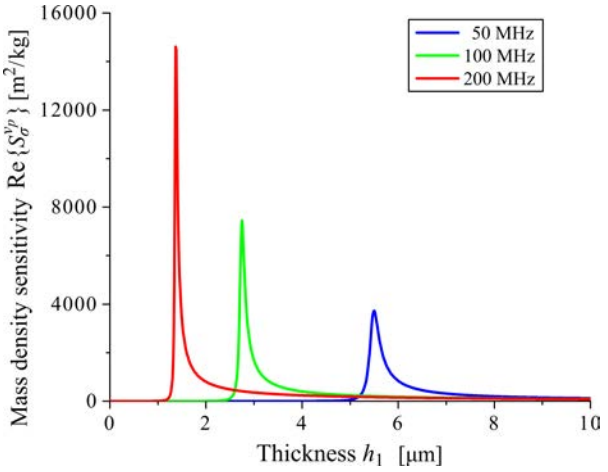

Fig. 5. Real part of the mass density sensitivity $S_\sigma^{v_p}$ [m^2/kg] for Love surface waves propagating in PMMA – Diamond waveguides, loaded with a thin lossless film with the surface mass density σ, as a function of thickness h_1 of the PMMA guiding surface layer, for different values of wave frequency f = 50, 100, and 200 MHz.

It is apparent that the real part of the mass density sensitivity $S_\sigma^{v_p}$ displays resonant like peaks, as a function of both f and h_1 and it drops gradually to zero for higher frequencies if $f \to +\infty$.

Next, we also analysed a Love wave sensor employing a waveguide with a diamond substrate. Figures 4 and 5 show dependencies of the real part of the mass density sensitivity $S_\sigma^{v_p}$ as a function of frequency f and thickness h_1 for the PMMA surface layer deposited this time on a diamond substrate.

We used a diamond substrate because the velocity of the bulk shear wave in it is very high (12 823 m/s). In the waveguide, the PMMA surface layer deposited on a diamond substrate, we can observe a very large contrast of the SH bulk wave velocities (1100 m/s in PMMA and 12 823 m/s in diamond), which should result in a very high sensitivity.

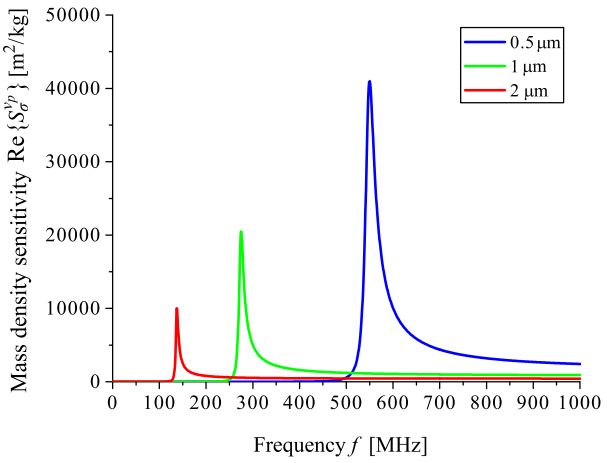

Fig. 4. Real part of the mass density sensitivity $S_\sigma^{v_p}$ [m^2/kg] for Love surface waves propagating in PMMA – Diamond waveguides loaded with a thin lossless film with the mass surface density σ, as a function of Love wave frequency f, for different values of thickness h_1 of the guiding PMMA surface layer (h_1 = 0.5, 1, and 2 μm).

Indeed, Love wave sensors based on PMMA on Diamond structures have a significantly larger mass sensitivity (five times) than sensors using PMMA on Quartz structures.

6. Conclusions

From the theoretical analysis and numerical calculations performed in this work, we can draw the following conclusions:

1) the real part of the mass density sensitivity $S_\sigma^{v_p}$ of Love wave sensors can be optimised (maximised) by proper selection of material and geometric parameters of the layered waveguide structure;
2) for a constant frequency f, the real part of the mass density sensitivity $S_\sigma^{v_p}$ reaches a maximum as a function of thickness h_1 of the surface layer;
3) for a constant thickness h_1 of the surface layer, the real part of the mass density sensitivity attains a maximum as a function of frequency f;
4) the real part of the mass density sensitivity $S_\sigma^{v_p}$ of the Love wave sensors increases with growing velocity ratio v_2/v_1^0, where v_1^0 is the bulk shear wave velocity in the surface layer, and v_2 is the bulk shear wave velocity in the substrate;
5) a more complete optimisation process of the mass density sensitivity $S_\sigma^{v_p}$ of Love wave sensors requires further theoretical and numerical investigations.

Acknowledgment

The project was funded by the National Science Centre (Poland), granted on the basis of Decision No. 2016/21/B/ST8/02437.

References

1. Achenbach J.D. (1973), *Wave Propagation in Elastic Solids*, North-Holland, Amsterdam.

2. Auld B.A. (1990), *Acoustic Fields and Waves in Solids*, Vol. II, Krieger Publishing Company, Florida.

3. Ballantine D.S. *et al.* (1997), *Acoustic Wave Sensors. Theory, Design, and Physico-Chemical Applications*, Academic Press, San Diego.

4. Chen X., Liu D. (2010), Analysis of viscosity sensitivity for liquid property detection applications based on SAW sensors, *Materials Science and Engineering C*, **30**(8): 1175–1182, doi: 10.1016/j.msec.2010.06.008.

5. Chu S-Y., Water W., Liaw J-T. (2003), An investigation of the dependence of ZnO film on the sensitivity of Love mode sensor in ZnO/quartz structure, *Ultrasonics*, **41**(2): 133–139, doi: 10.1016/S0041-624X(02)00430-4.

6. El Baroudi A., Le Pommellec J.Y. (2019), Viscoelastic fluid effect on the surface wave propagation, *Sensors & Actuators A: Physical*, **291**: 188–195, doi: 10.1016/j.sna.2019.03.039.

7. Haskell N.A. (1953), The dispersion of surface waves on multilayered media, *Bulletin of the Seismological Society of America*, **43**(1): 17–34.

8. Ke G.H., Dong H., Kristensen M., Thompson M. (2011), Modified Thomson Haskell matrix methods for surface-wave dispersion-curve calculation and their accelerated root-searching schemes, *Bulletin of the Seismological Society of America*, **101**(4): 1692–170, doi: 10.1785/0120100187.

9. Kiełczyński P., Pajewski W., Szalewski M. (1998), Piezoelectric sensors for investigations of microstructures, *Sensors and Actuators A: Physical*, **65**(1): 13–18, doi: 10.1016/S0924-4247(98)80003-4.

10. Kiełczyński P., Szalewski M. (2011), An inverse method for determining the elastic properties of thin layers using Love surface waves, *Inverse Problems in Sciences and Engineering*, **19**(1): 31–43, doi: 10.1080/17415977.2010.531472.

11. Kiełczyński P. *et al.* (2014a), Application of ultrasonic wave celerity measurement for evaluation of physicochemical properties of olive oil at high pressure and various temperatures, *LWT – Food Science and Technology*, **57**(1): 253–259, doi: 10.1016/j.lwt.2014.01.027.

12. Kiełczyński P. *et al.* (2014b), Determination of physicochemical properties of diacylglycerol oil at high pressure by means of ultrasonic methods, *Ultrasonics*, **54**: 2134–2140, doi: 10.1016/j.ultras.2014.06.013.

13. Kiełczyński P., Szalewski M., Balcerzak A. (2014c), Inverse procedure for simultaneous evaluation of viscosity and density of Newtonian liquids from dispersion curves of Love waves, *Journal of Applied Physics*, **116**(4): 044902 (7), doi: 10.1063/1.4891018.

14. Kiełczyński P., Szalewski M., Balcerzak A., Wieja K., Rostocki A.J., Siegoczyński R.M. (2015a), Ultrasonic evaluation of thermodynamic parameters of liquids under high pressure, *IEEE Transactions on Ultrasonics, Ferroelectrics, and Frequency Control*, **62**(6): 1122–1131, doi: 10.1109/TUFFC.2015.007053.

15. Kiełczyński P., Szalewski M., Balcerzak A., Wieja K. (2015b), Group and phase velocity of Love waves propagating in elastic functionally graded materials, *Archives of Acoustics*, **40**(2): 273–281, doi: 10.1515/aoa-2015-0030.

16. Kiełczyński P., Szalewski M., Balcerzak A., Wieja K. (2016), Propagation of ultrasonic Love wave in non-homogeneous elastic functionally graded materials, *Ultrasonics*, **65**: 220–227, doi: 10.1016/j.ultras.2015.10.001.

17. Kiełczyński P. (2018), Direct Sturm–Liouville problem for surface Love waves propagating in layered viscoelastic waveguides, *Applied Mathematical Modelling*, **53**: 419–432, doi: 10.1016/j.apm.2017.09.013.

18. Kushibiki J., Takanaga I., Nishiyama S. (2002), Accurate measurements of the acoustical physical constants of synthetic α-quartz for SAW devices, *IEEE Transactions on Ultrasonics, Ferroelectrics, and Frequency Control*, **49**(1): 125–135, doi: 10.1109/58.981390.

19. Liu J.-S., Wang L.-J., He S.-T. (2015), On the fundamental mode Love wave devices incorporating thick viscoelastic layers, *Chinese Physics Letters*, **32**: 064301 (3 pages), doi: 10.1088/0256-307X/32/6/064301.

20. Mortet V., Williams O. A., Haenen K. (2008), Diamond: a material for acoustic devices, *Physica Status Solidi (a)*, **205**(5): 1009 – 1020, doi: 10.1002/pssa.200777502.

21. Pajewski W., Kiełczyński P., Szalewski M. (1998), Resonant piezoelectric ring transformer, *IEEE Ultrasonics Symposium*, Sendai, Japan, October 5–8, pp. 977–980.

22. Rasmusson A., Gizeli E. (2001), Comparison of poly(methylmethacrylate) and Novolak waveguide coatings for an acoustic biosensor, *Journal of Applied Physics*, **90**(12): 5911–5914, doi: 10.1063/1.1405142.

23. Raum K., Brandt J. (2003), Simultaneous determination of acoustic impedance, longitudinal and lateral wave velocities for the characterization of the elastic microstructure of cortical bone, *World Congress on Ultrasonics*, Paris, September 7–10, pp. 321–324.

24. Rocha Gaso M.I., Jiménez Y., Francis L.A., Arnau A. (2013), Love wave biosensors: A review, [in:] *State of the Art in Biosensors*, Rinken T. [Ed.], Rijeka: IntechOpen, doi: 10.5772/53077.

25. Rose J.L. (2014), *Ultrasonic Guided Waves in Solid Media*, Cambridge: Cambridge University Press.

26. Takayanagi K., Kondoh J. (2018), Improvement of estimation method for physical properties of liquid using shear horizontal surface acoustic wave sensor response, *Japaneese Journal of Applied Physics*, **57**: 07LD02 (7 pages), doi: 10.7567/JJAP.57.07LD02.

27. Vikström A., Voinova M.V. (2016), Soft-film dynamics of SH-SAW sensors in viscous and viscoelastic fluids, *Sensing and Bio-sensing Research*, **11**(Part 2): 78–85, doi: 10.1016/j.sbsr.2016.08.004.

28. Thomson W.T. (1950), Transmission of elastic waves through a stratified solid medium, *Journal of Applied Physics*, **21**(2): 89–93, doi: 10.1063/1.1699629.

29. Wu H., Xiong X., Zu H., Wang J.H.-C., Wang Q.-M. (2017), Theoretical analysis of a Love wave biosensor in liquid with a viscoelastic wave guiding layer, *Journal of Applied Physics*, **121**(5): 054501 (13 pages), doi: 10.1063/1.4975112.

30. Xu Z., Yuan Y.J. (2018), Implementation of guiding layers of surface acoustic wave devices: A review, *Biosensors and Bioelectronics*, **99**: 500–512, doi: 10.1016/ j.bios.2017.07.060